ELSEVIER

Engineering Structures 23 (2001) 622–630

ENGINEERING STRUCTURES

www.elsevier.com/locate/engstruct

Beat phenomenon in combined structure-liquid damper systems

Swaroop K. Yalla [a,*], Ahsan Kareem [b]

[a] *NatHaz Modeling Laboratory, Department of Civil Engineering and Geological Sciences, University of Notre Dame, Notre Dame, IN 46556, USA*

[b] *Department of Civil Engineering and Geological Sciences, University of Notre Dame, Notre Dame, IN 46556, USA*

Received 21 December 1999; received in revised form 30 June 2000; accepted 9 July 2000

Abstract

The classical *beat phenomenon* has been observed in most combined structure-liquid damper systems. The focus of this paper is to provide a better understanding of this phenomenon, which is caused by the coupling that is introduced through the mass matrix of the combined system. However, beyond a certain level of damping in the secondary system (liquid damper), the *beat phenomenon* ceases to exist. This is due to coalescing of the modal frequencies of the combined system to a common frequency beyond a certain level of damping in the secondary system. Numerical and experimental results are presented in this paper to elucidate the *beat phenomenon* in combined structure-liquid damper systems.

Keywords: Nonlinear dynamics; *Beat phenomenon*; Combined systems; Coupled systems; Liquid dampers; Free vibrations

1. Introduction

The effectiveness of liquid dampers in controlling structural motions under wind and earthquake loadings has been demonstrated in theory and practice. The most commonly used liquid dampers include Tuned Sloshing Dampers (TSDs) and Tuned Liquid Column Dampers (TLCDs). The TSD is a type of inertial mass damper in which the secondary system is represented by a sloshing liquid mass in a container [2,3]. Damping in TSDs results from wave breaking and the impact of liquid on the container walls [7]. The TLCD is a liquid damper in which an oscillating liquid column in a U-tube container serves as the secondary inertial mass [5]. Damping in TLCDs is introduced by an orifice provided in the U-tube to dampen the oscillations of the liquid column.

Experimental studies involving a TLCD combined with a simple structure have provided insightful understanding of the behavior of liquid damper systems (Fig. 1). The motivation of this paper is portrayed in Fig. 2(a) and (b), which shows the free vibration decay of a combined structure-TSD and -TLCD in the laboratory. The controlled response exhibits the classical *beat phenomenon* characterized by a modulated instead of an exponential decay in the signature. The *beat phenomenon* has been discussed in many classical texts on vibration (e.g., [1]). There is a transfer of energy between the coupled system, similar to the coupled penduli problem. This paper focuses on better understanding the *beat phenomenon* for the combined structure-TLCD system.

The free vibration equations of motion of the combined single degree of freedom structure (primary system) and TLCD (secondary system) shown in Fig. 3(c) are given by,

$$\begin{bmatrix} m_1+m_2 & \alpha m_2 \\ \alpha m_2 & m_2 \end{bmatrix}\begin{bmatrix} \ddot{x}_1 \\ \ddot{x}_2 \end{bmatrix}+\begin{bmatrix} c_1 & 0 \\ 0 & c_2|\dot{x}_2| \end{bmatrix}\begin{bmatrix} \dot{x}_1 \\ \dot{x}_2 \end{bmatrix}+\begin{bmatrix} k_1 & 0 \\ 0 & k_2 \end{bmatrix}\begin{bmatrix} x_1 \\ x_2 \end{bmatrix} = \begin{bmatrix} 0 \\ 0 \end{bmatrix} \quad (1)$$

where x_1 and x_2 are the displacement of the primary system with respect to the fixed base and the displacement of the liquid in the secondary system, respectively; m_2=mass of fluid in the tube=ρAl; c_2=nonlinear damping coefficient of the liquid damper; k_2=stiffness of the liquid column=$2\rho Ag$; m_1, k_1, c_1=mass, stiffness and damping coefficient of the structure; ρ=mass density of liquid; A=cross sectional area of the tube; g=gravitational accel-

* Corresponding author. Tel.: +1-219-631-4307; fax: +1-219-631-9236.

E-mail address: swaroop.k.yalla.1@nd.edu (S.K. Yalla).

0141-0296/01/$ - see front matter
PII: S0141-0296(00)00085-7

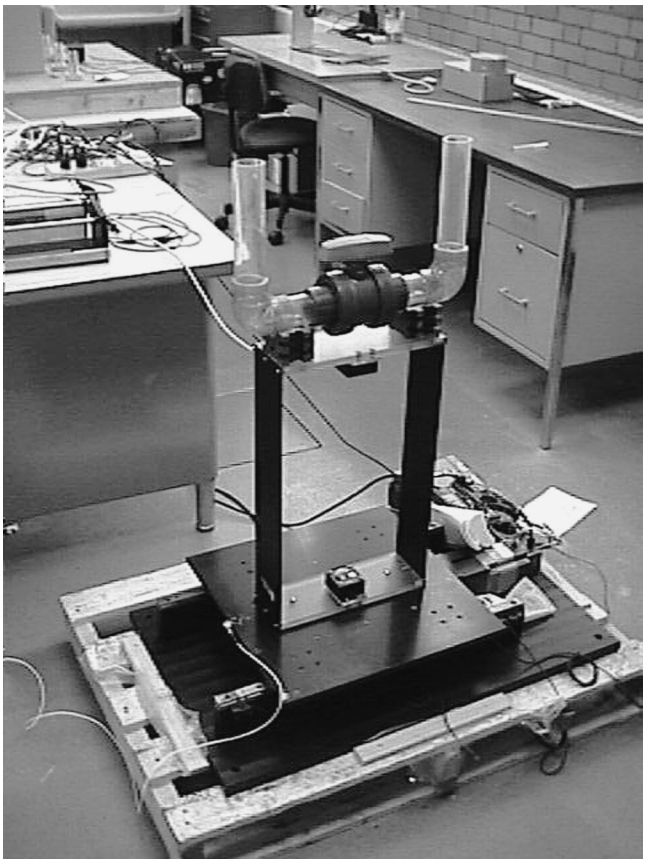

Fig. 1. Experimental setup for combined structure-TLCD system on a shaking table.

eration; α is the length ratio=b/l; l=total length of the water column; and b=horizontal length of the column. Details of this system can be found in [6]. The behavior of the general combined system of Fig. 3(c), as well as the two special cases of Fig. 3(a) and (b), are examined in the rest of this paper.

2. Behavior of SDOF system with TLCD

2.1. Case 1: undamped combined system

The coupled equations of motion without damping in the primary and secondary system (Fig. 3(a)) can be obtained from Eq. (1) by setting c_1 and c_2 equal to zero,

$$\begin{bmatrix} 1+\mu & \alpha\mu \\ \alpha & 1 \end{bmatrix}\begin{bmatrix} \ddot{x}_1 \\ \ddot{x}_2 \end{bmatrix}+\begin{bmatrix} \omega_1^2 & 0 \\ 0 & \omega_2^2 \end{bmatrix}\begin{bmatrix} x_1 \\ x_2 \end{bmatrix}=\begin{bmatrix} 0 \\ 0 \end{bmatrix} \tag{2}$$

where μ is the mass ratio=m_2/m_1; ω_1 is the natural frequency of the structure; and $\omega_2=\sqrt{2g/l}$ is the natural frequency of the damper. The modal frequencies of this system are given by:

$$\bar{\omega}_{1,2}=\sqrt{\frac{\omega_1^2+\omega_2^2(1+\mu)\pm\Pi}{2(1+\mu-\alpha^2\mu)}} \tag{3}$$

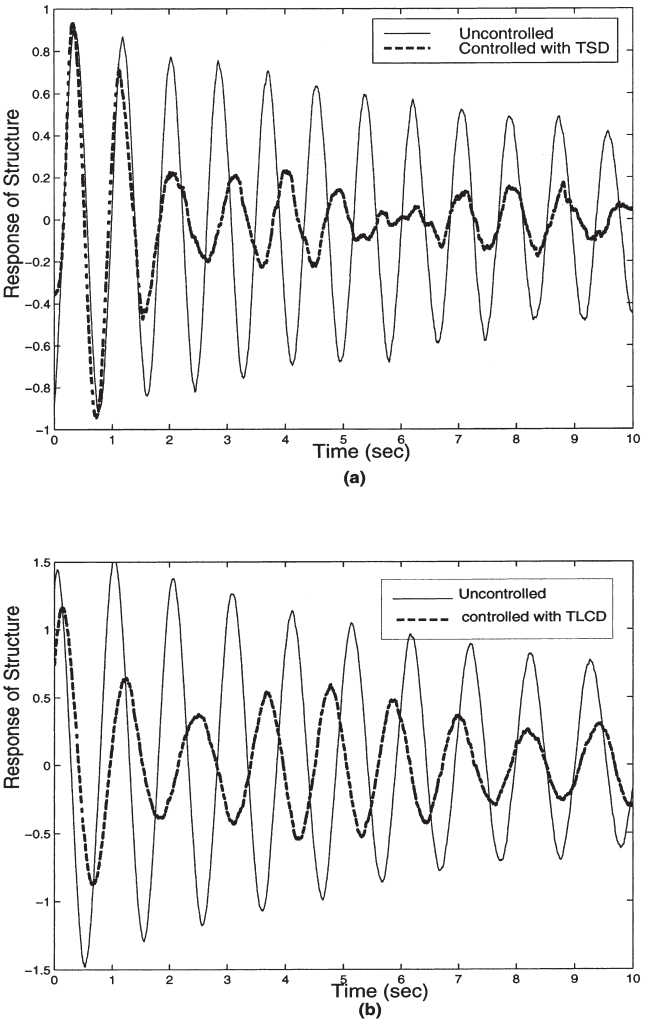

Fig. 2. Uncontrolled and controlled response of a structure combined with (a) TSD (b) TLCD.

where $\Pi^2=(\omega_1^2-\omega_2^2(1+\mu))^2+4\omega_1^2\omega_2^2\alpha^2\mu$.

It is obvious from Eq. (3) that, for an uncoupled system (i.e., for α=0), the eigenvalues reduce to:

$$\bar{\omega}_1=\frac{\omega_1}{\sqrt{1+\mu}};\bar{\omega}_2=\omega_2 \tag{4}$$

The coupling parameter α in the mass matrix is responsible for the *beat phenomenon*. Fig. 4 shows the phase plane portraits for the primary system for different values of α. Unless mentioned otherwise, all units of displacements, frequencies and velocities are m, rad/sec and m/sec, respectively. The first portrait shows that with no coupling there is only one frequency at which the structure responds, and as the coupling parameter increases there is *interference* between the two states of the primary system, namely, x_1 and $\dot{x}_1$.

For all simulations in this paper, the following parameters have been kept constant, ω_1=1 Hz, μ=0.01 and ω_2=0.99 Hz. Fig. 5 shows the time histories of the dis-

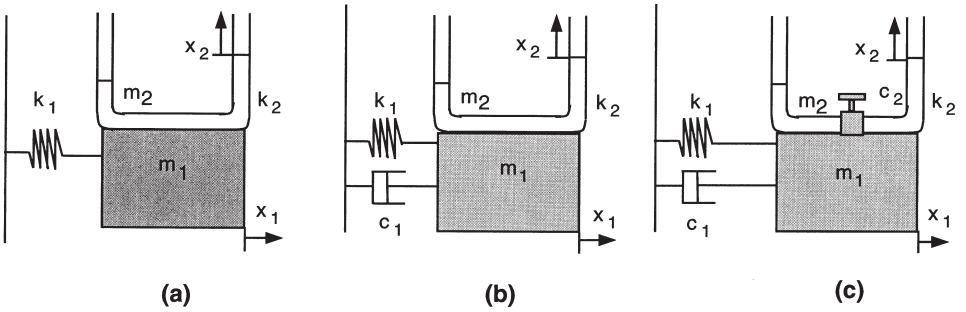

Fig. 3. Different combined systems.

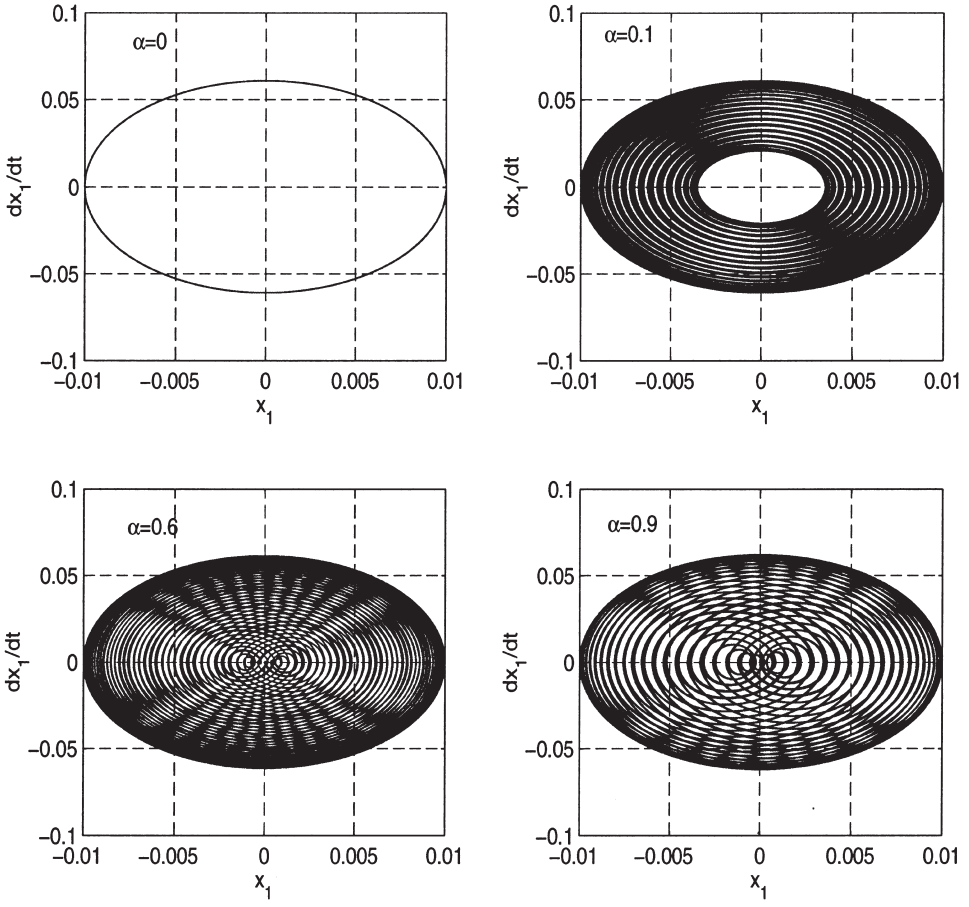

Fig. 4. Phase plane portraits of the undamped coupled system.

placement of the undamped primary system for α=0 and α=0.6. When coupling is present between the two systems, the displacement signature is amplitude modulated.

To understand this phenomenon better, one can consider the solution of the system of equations given in Eq. (2). After some mathematical manipulation the displacement of the primary system for the initial conditions, $x_1(0)=x_0$; $x_2(0)=0$; $\dot{x}_1(0)=0$ and $\dot{x}_2(0)=0$, is given by:

$$x_1(t)=x_0\cos\left(\frac{\omega_B t}{2}\right)\cos\left(\frac{\omega_A t}{2}\right) \tag{5}$$

where $\omega_A=\bar{\omega}_1+\bar{\omega}_2$ and $\omega_B=\bar{\omega}_2-\bar{\omega}_1$, which means that the resulting function is an amplitude-modulated harmonic function with a frequency equal to ω_B and the amplitude varying with a frequency of ω_A. This undamped combined system case has been examined in texts on vibration (e.g., [1]).

2.2. Case 2: linearly damped structure with undamped secondary system

In this section, a linearly damped primary system with undamped secondary system as shown in Fig. 3(b) is

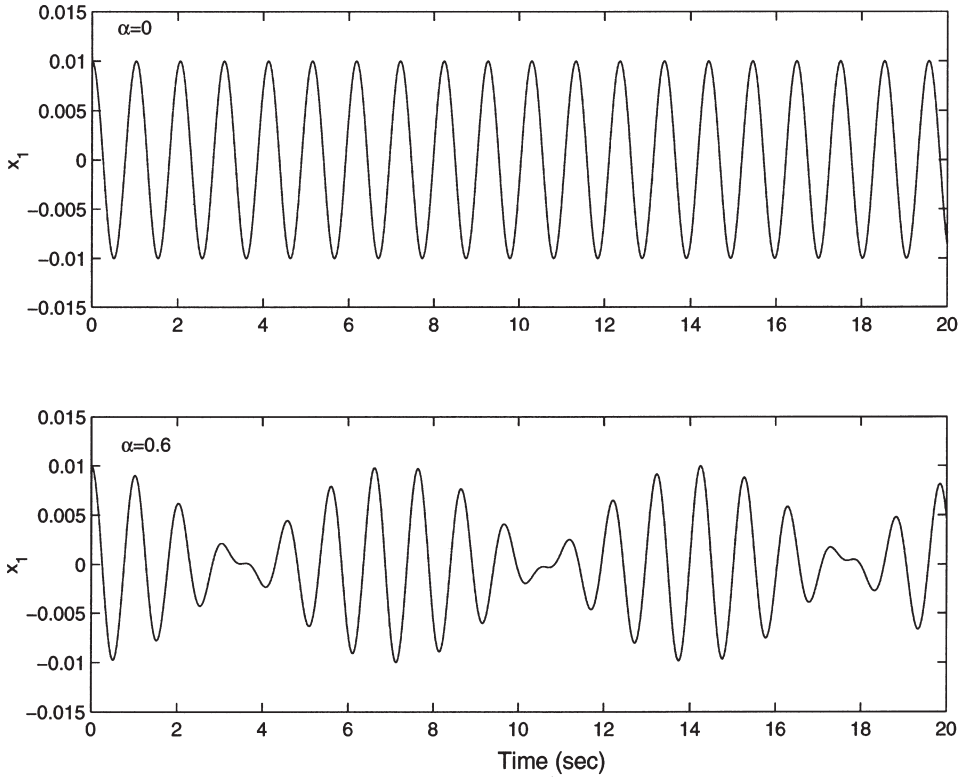

Fig. 5. Time histories of primary system displacement for α=0 and α=0.6.

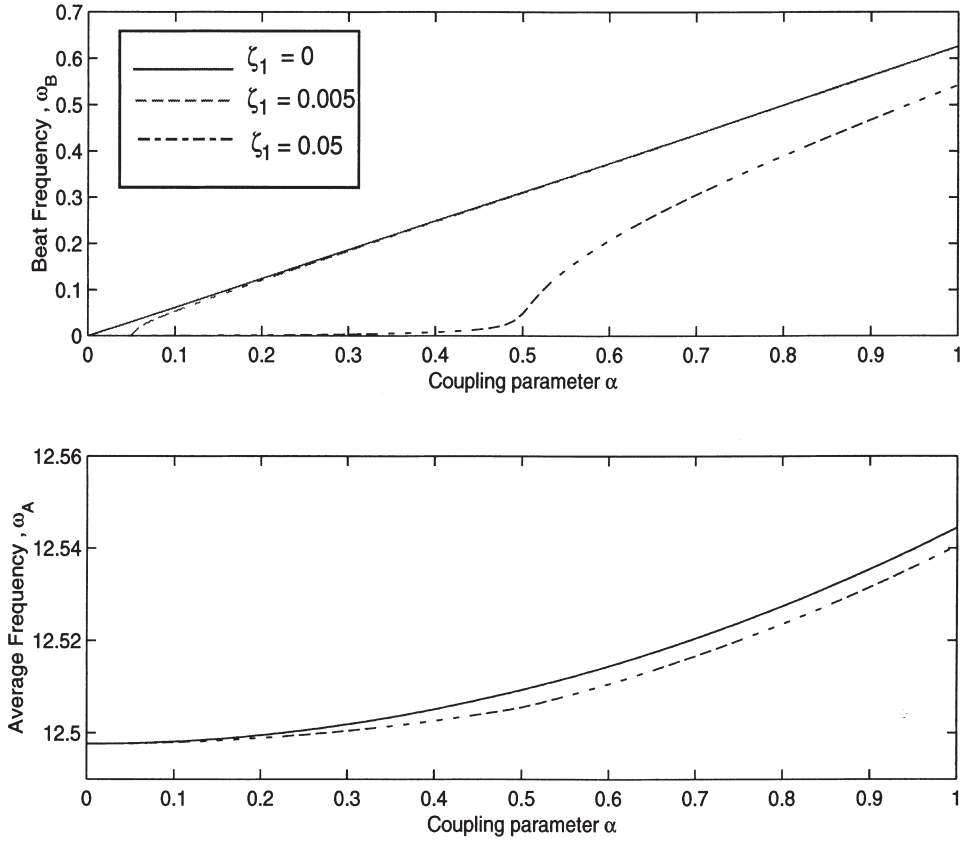

Fig. 6. Variation of ω_A and ω_B as a function of α.

considered. Accordingly, the equations of motion are given by:

$$\begin{bmatrix}1+\mu & \alpha\mu\\ \alpha & 1\end{bmatrix}\begin{bmatrix}\ddot{x}_1\\ \ddot{x}_2\end{bmatrix}+\begin{bmatrix}2\omega_1\zeta_1 & 0\\ 0 & 0\end{bmatrix}\begin{bmatrix}\dot{x}_1\\ \dot{x}_2\end{bmatrix}+\begin{bmatrix}\omega_1^2 & 0\\ 0 & \omega_2^2\end{bmatrix}\begin{bmatrix}x_1\\ x_2\end{bmatrix} \quad (6)$$
$$=\begin{bmatrix}0\\ 0\end{bmatrix}$$

This system has two complex conjugate pairs of eigenvalues,

$$\lambda_{1,2}=-\bar{\omega}_1\tilde{\zeta}_1\pm i\bar{\omega}_1\sqrt{1-\tilde{\zeta}_1^2}\text{ and }\lambda_{3,4}=-\bar{\omega}_2\tilde{\zeta}_2\pm i\bar{\omega}_2\sqrt{1-\tilde{\zeta}_2^2}$$

where $\omega_{1,2}$ are the modal frequencies and $\tilde{\zeta}_{1,2}$ are the modal damping ratios. The average frequency and the beat frequency are plotted in Fig. 6 for different damping ratios of the primary system. At α=0 the beat frequency (i.e. the difference in modal frequencies) tends to be zero. As the coupling is increased there is an increase in the beat frequency which causes the *beat phenomenon*. From this analysis, one can conclude that there is no *beat phenomenon* when the difference in the modal frequencies approaches zero. Fig. 6 also shows the effect of introducing damping in the primary system. At high levels of damping ratio, there is a wider range of coupling term α which results in the beat frequency being equal to zero. This means that, over this range of the coupling term, there is hardly any *beat phenomenon*. For α=0.3, *beat phenomenon* is present when the damping ratio in the primary system is 0.005, but it disappears when the damping ratio is 0.05. Fig. 7 shows the effect of damping in the primary system on the response of the primary system. As the damping ratio increases, the response dies out in an exponential decay. However, the *beat phenomenon* still exists. This poses difficulty in the estimation of system damping from free vibration response time histories.

At this stage, the effect of a decrease in beat frequency on the response signal can be further examined. Fig. 8 shows that as ω_B approaches zero, T_B (the time period of the beat frequency) becomes very large. The parameter influencing the decay function is Ψ (for a SDOF system, $\Psi=\zeta_1\omega_1$). As a result, due to the damping in the primary system, the response dies out before the next peak of the beat cycle arises. Therefore, the response resembles that of a damped single degree of freedom (SDOF) system.

2.3. Case 3: damped primary and secondary system

In this section, the system represented by Fig. 3(c) is considered, where now an orifice in the middle of the U-tube imparts damping to the system. In this case, the following equations of motion apply:

$$\begin{bmatrix}1+\mu & \alpha\mu\\ \alpha & 1\end{bmatrix}\begin{bmatrix}\ddot{x}_1\\ \ddot{x}_2\end{bmatrix}+\begin{bmatrix}2\omega_1\zeta_1 & 0\\ 0 & \omega_2^2\xi|\dot{x}_2|/4g\end{bmatrix}\begin{bmatrix}\dot{x}_1\\ \dot{x}_2\end{bmatrix} \quad (7)$$

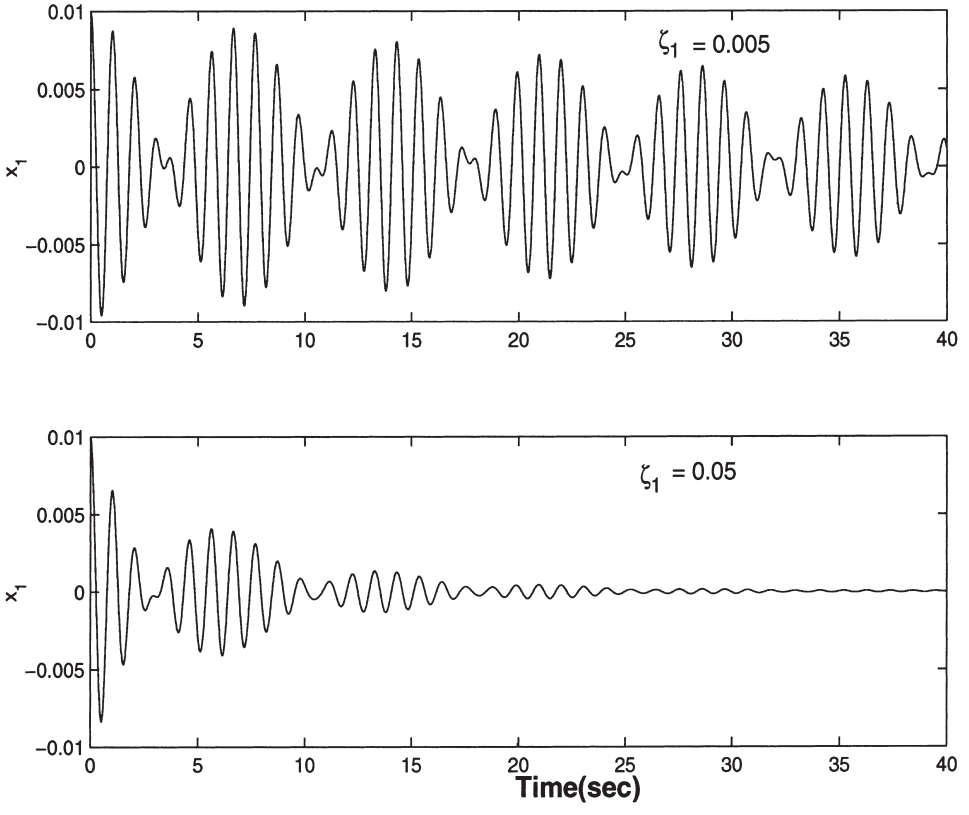

Fig. 7. Time histories of response for ζ_1=0.005 and ζ_1=0.05.

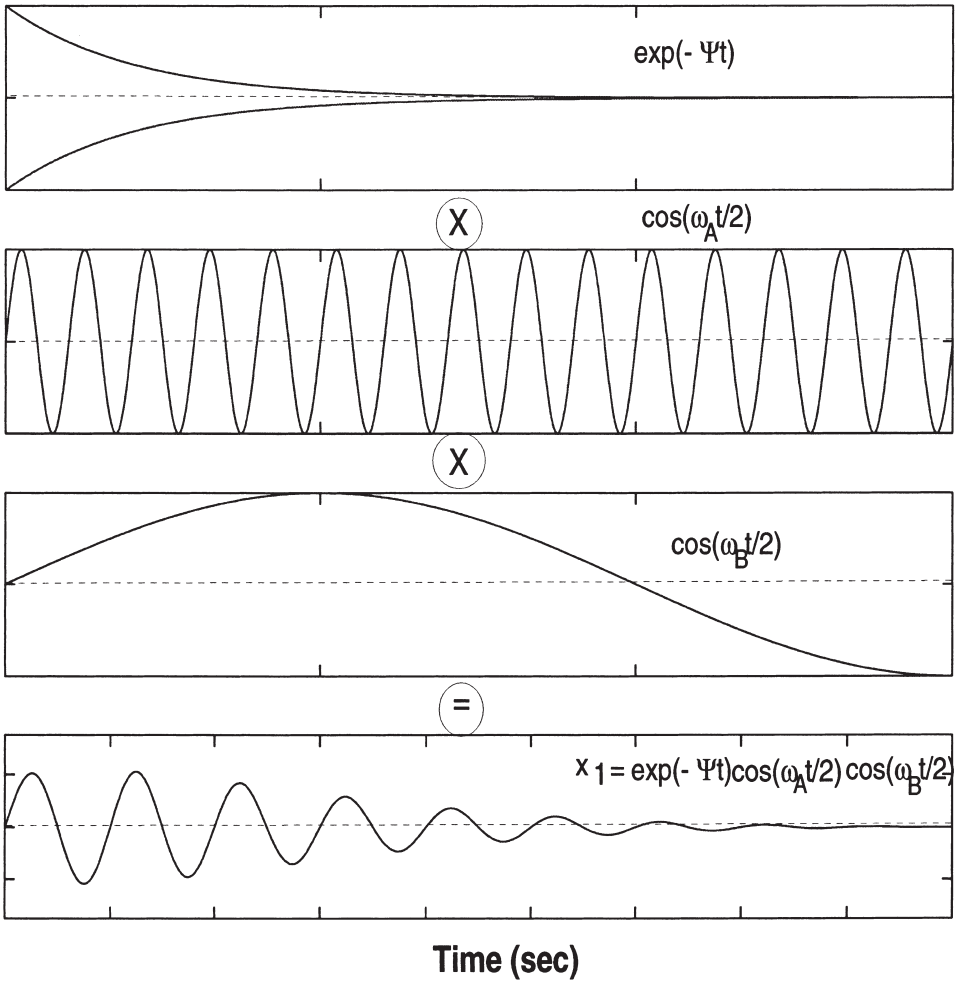

Fig. 8. Anatomy of the damped response signature.

$$+\begin{bmatrix}\omega_1^2 & 0\\ 0 & \omega_2^2\end{bmatrix}\begin{bmatrix}x_1\\ x_2\end{bmatrix}=\begin{bmatrix}0\\ 0\end{bmatrix}$$

where ξ is the headloss coefficient and $c_2=\frac{1}{2}\rho A\xi$. Eq. (7) is numerically integrated at different levels of the headloss coefficient and setting $\zeta_1=0.001$ and $\alpha=0.3$ (Fig. 9). The figure shows an interesting behavior of the liquid damper system. In the previous section, the damping simply caused an exponential decay of the beat response. However, in this case, the *beat phenomenon* disappears after a certain level of the headloss coefficient. Since an analytical solution is not convenient for this equation due to the quadratic nonlinearity in the damping associated with the secondary system, a linearized version of this system is generally considered. Therefore, Eq. (7) is recast as:

$$\begin{bmatrix}1+\mu & \alpha\mu\\ \alpha & 1\end{bmatrix}\begin{bmatrix}\ddot{x}_1\\ \ddot{x}_2\end{bmatrix}+\begin{bmatrix}2\omega_1\zeta_1 & 0\\ 0 & 2\omega_2\zeta_2\end{bmatrix}\begin{bmatrix}\dot{x}_1\\ \dot{x}_2\end{bmatrix} \tag{8}$$

$$+\begin{bmatrix}\omega_1^2 & 0\\ 0 & \omega_2^2\end{bmatrix}\begin{bmatrix}x_1\\ x_2\end{bmatrix}=\begin{bmatrix}0\\ 0\end{bmatrix}$$

The linearization of this system is based on harmonic motion of the system. For a quadratic non-linearity, the equivalent damping ratio can be obtained [4]. For a quadratic nonlinearity of the form,

$$F=c_2|\dot{x}|\dot{x} \tag{9}$$

where F is the damping force, the equivalent linear damping is given as:

$$C_e=\frac{8c_2A_{x_2}\omega_2}{3\pi} \tag{10}$$

where A_{x2} is the amplitude of liquid displacement. After some manipulation, one can obtain an expression for the equivalent damping ratio:

$$\zeta_2=\frac{\xi\omega_2^2A_{x_2}}{3\pi^2} \tag{11}$$

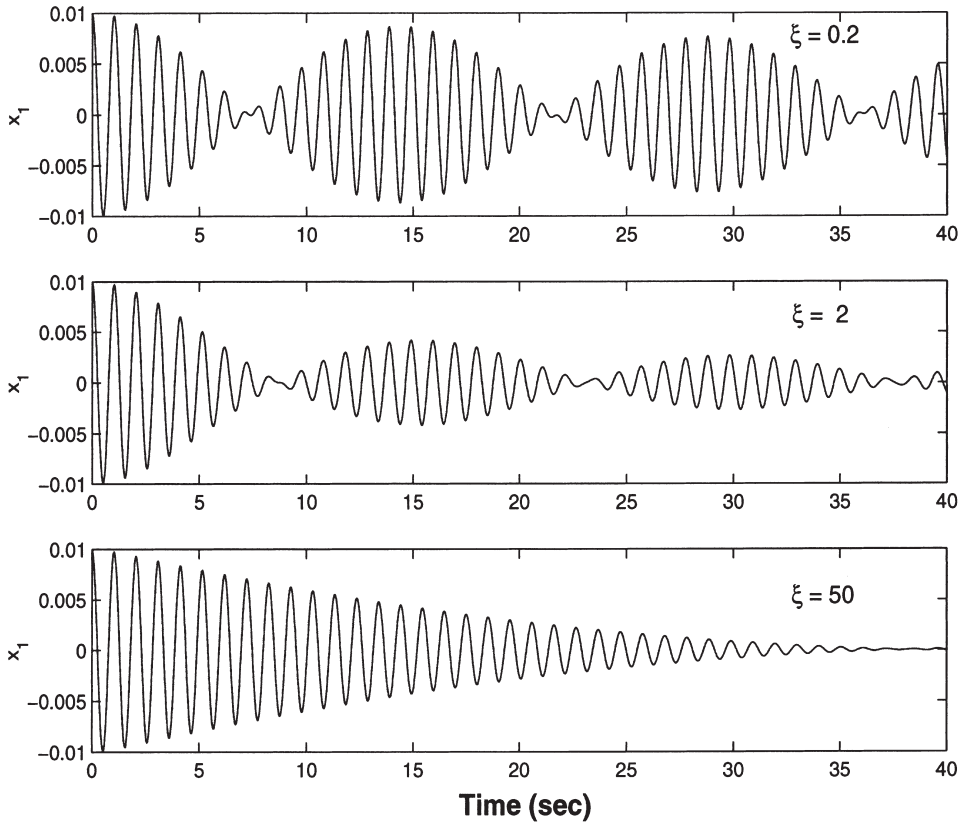

Fig. 9. Time histories of response for ξ=0.2, 2 and 50.

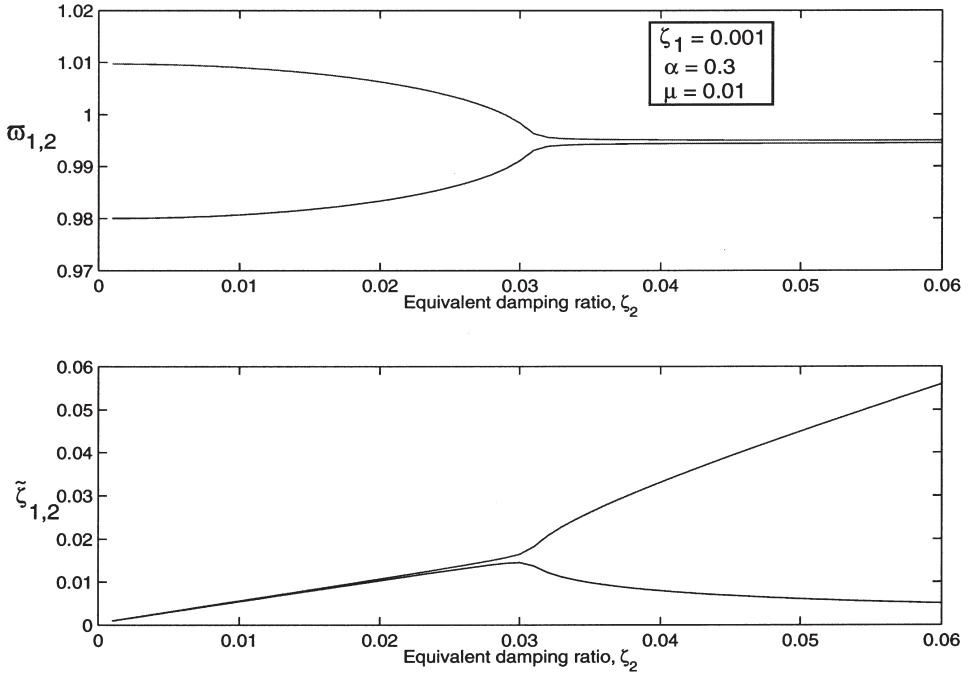

Fig. 10. Modal frequencies and modal damping ratios of combined system as a function of the damping ratio of the TLCD.

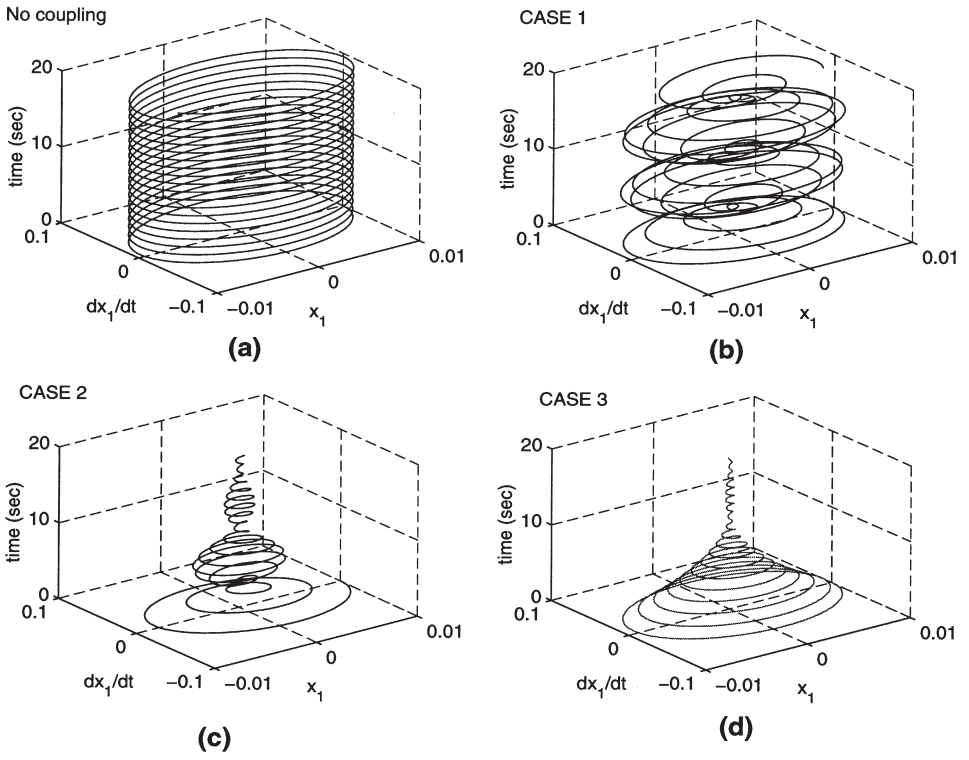

Fig. 11. Phase–plane 3D plots (a) uncoupled system (b) case 1: undamped system (c) case 2: system with damping in primary system only (d) case 3: system with damping in both primary and secondary systems.

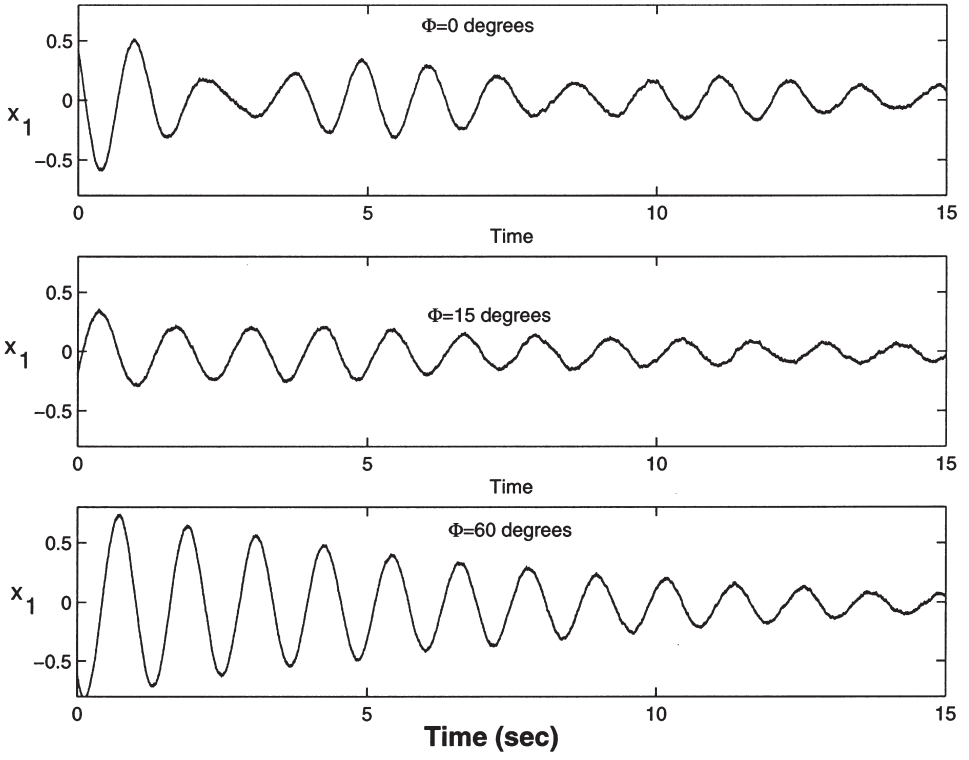

Fig. 12. Experimental free vibration response with different orifice openings (Φ=0 fully open).

Similar expressions can be derived for random response cases.

The modal frequencies and damping ratios of the system defined in Eq. (8) are plotted in Fig. 10 as a function of equivalent damping ratio ζ_2, which was defined in Eq. (11). Fig. 10 explains the disappearance of the *beat phenomenon* due to coalescing of the modal frequencies after a certain value of the headloss coefficient, ξ, (which is related to ζ_2 by Eq. (11)) is reached. The resulting beat frequency approaches zero and hence *beat phenomenon* ceases to exist. This is similar to a previous case where there was no *beat phenomenon* for coupling term α=0, in which case the beat frequency was also zero.

Fig. 11 shows three dimensional plots of state space portraits as a function of time. Fig. 11(a) shows the evolution for an uncoupled system in which the amplitude of response is constant. Fig. 11(b) and (c) show the cases discussed in Sections 2.1 and 2.2. The final plot, Fig. 11(d), shows case 3 in which no *beat phenomenon* occurs in the coupled system. The *beat phenomenon* can also be examined from the wave propagation viewpoint. The *spatial interference phenomenon* is well understood in the context of sound waves, light waves and water waves which all exhibit interference patterns in space. A ripple tank is a common tool used to demonstrate the spatial interference phenomenon with the locations of constructive and destructive interference. One can readily see the similarity of the two phenomena, namely the *beat phenomenon* and the spatial interference phenomenon. The state–space portraits in Figs. 4 and 11 show similar interference patterns.

In order to further validate the observations made in this paper, a simple experiment was conducted using the experimental setup shown in Fig. 1. The TLCD was designed with a variable orifice, to effectively change the headloss coefficient. At Φ=0 degrees, the valve is fully opened and the headloss is increased with an increase in the angle of rotation, Φ. In Fig. 12, there is an obvious beat pattern for low headloss coefficients. However, as the headloss coefficient is increased, the *beat phenomenon* disappears and an exponentially decaying signature is obtained. A similar observation was made in Fig. 9 for simulated time histories.

3. Conclusions

Similar to coupled mechanical systems, the combined structure-liquid damper system exhibits the *beat phenomenon* due to the coupling term that appears in the mass matrix of the combined system. The free vibration structural response resembles an amplitude modulated signal. The beat frequency of the modulated signature is given by the difference in the modal frequencies of the coupled system. However, beyond a certain level of damping in the secondary system (liquid damper), the *beat phenomenon* ceases to exist. This is attributed to the coalescing of the modal frequencies of the combined system to a common frequency beyond a certain level of damping in the secondary system.

Acknowledgements

The authors gratefully acknowledge the support provided by NSF Grant CMS–9503779.

References

[1] Den Hartog JP. Mechanical vibrations. 4th ed. New York: McGraw-Hill, 1956.
[2] Modi VJ, Welt F. Vibration control using nutation dampers. In: King R, editor, International conference on Flow induced Vibrations. London: BHRA, 1987.
[3] Kareem A, Sun WJ. Stochastic response of structures with fluid-containing appendages. J Sound and Vibrat 1987;119(3):389–408.
[4] Roberts JB, Spanos PD. Random vibration and statistical linearization. New York: Wiley, 1990.
[5] Sakai F, Takaeda S. Tuned liquid column damper — new type device for suppression of building vibrations. Proceedings International Conference on High Rise Buildings, Nanjing, China, March 1989.
[6] Yalla SK, Kareem A, Kantor JC. Semi-active control strategies for tuned liquid column dampers to reduce wind and seismic response of structures. Proceedings of Second World Conference on Structural Control, Kyoto, Japan, June 1998.
[7] Yalla SK, Kareem A. Modelling tuned liquid dampers as sloshing–slamming dampers. Proceedings of the 10th International Conference on Wind Engineering, Copenhagen, Denmark, June 1999.